



Published in final edited form as:

J Biomol Screen. 2009 July ; 14(6): 596–609. doi:10.1177/1087057109335671.

Detection of Intracellular Granularity Induction in Prostate Cancer Cell Lines by Small Molecules Using the HyperCyt® High-Throughput Flow Cytometry System

MARK K. HAYNES^{1,2}, J. JACOB STROUSE^{1,2}, ANNA WALLER^{1,2}, ANDREI LEITAO^{1,3}, RAMONA F. CURPAN^{1,3}, CRISTIAN BOLOGA^{1,3}, TUDOR I. OPREA^{1,3}, ERIC R. PROSSNITZ^{1,2,4}, BRUCE S. EDWARDS^{1,2,5}, LARRY A. SKLAR^{1,2,5}, and TODD A. THOMPSON⁶

¹University of New Mexico Center for Molecular Discovery, Albuquerque, New Mexico

²University of New Mexico Cancer Center, Albuquerque, New Mexico

³Division of Biocomputing, Department of Biochemistry and Molecular Biology, University of New Mexico Health Sciences Center, Albuquerque, New Mexico

⁴Department of Cellular Biology and Physiology, University of New Mexico Health Sciences Center, Albuquerque, New Mexico

⁵Department of Pathology, University of New Mexico Health Sciences Center, Albuquerque, New Mexico

⁶College of Pharmacy, University of New Mexico Health Sciences Center, Albuquerque, New Mexico

Abstract

Prostate cancer is a leading cause of death among men due to the limited number of treatment strategies available for advanced disease. Discovery of effective chemotherapeutics involves the identification of agents that inhibit cancer cell growth. Increases in intracellular granularity have been observed during physiological processes that include senescence, apoptosis, and autophagy, making this phenotypic change a useful marker for identifying small molecules that induce cellular growth arrest or death. In this regard, epithelial-derived cancer cell lines appear uniquely susceptible to increased intracellular granularity following exposure to chemotherapeutics. We have established a novel flow cytometry approach that detects increases in side light scatter in response to morphological changes associated with intracellular granularity in the androgen-sensitive LNCaP and androgen-independent PC3 human prostate cancer cell lines. A cell-based assay was developed to screen for small molecule inducers of intracellular granularity using the HyperCyt® high-throughput flow cytometry platform. Validation was performed using the Prestwick Chemical Library, where known modulators of LNCaP intracellular granularity, such as testosterone, were identified. Nonandrogenic inducers of granularity were also detected. A further screen of ~25,000 small molecules led to the identification of a class of aryl-oxazoles that increased intracellular granularity in both cell lines, often leading to cell death. The most potent agents exhibited submicromolar efficacy in LNCaP and PC3 cells.

© 2009 Society for Biomolecular Sciences

Address correspondence to: Mark K. Haynes, University of New Mexico Center for Molecular Discovery, 2325 Camino de Salud, CRF 221, MSC 116020, Albuquerque, NM 87131, MHaynes@salud.unm.edu.

Disclaimer: Larry A. Sklar and Bruce S. Edwards are founders of the company IntelliCyt that markets the HyperCyt technology.

Keywords

HyperCyt[®] high-throughput flow cytometry; small molecule screening; intracellular granularity; prostate cancer

Prostate cancer contributes significantly to cancer-related deaths in the United States. With the exception of skin cancer, prostate cancer is the most common malignancy in men, and its incidence has almost doubled over the last 3 decades.¹ While many of these identified neoplasms occur in elderly men and have a long doubling time, younger individuals often experience a more aggressive and life-threatening disease.² Prostatectomy and radiation therapy are useful treatment modalities for localized prostate cancer but are not effective for metastatic disease.^{3,4} Recurrent metastatic prostate cancers are initially treated with androgen ablation therapy. These treatments, which arose from the discovery that prostate cancer, at least in its initial stages, depends on androgen, consist of gonadotropin-releasing hormone agonists and direct androgen receptor antagonism.⁵ Unfortunately, as prostate cancer progresses, it invariably becomes refractory to androgen deprivation. Treatment options at this stage are severely limited and include chemotherapies, such as mitoxantrone or docetaxel, that only marginally increase lifespan. Clearly, new targets and drug screening methods are needed to facilitate the identification of novel therapeutic agents distinct from those associated with androgen ablation.

Increases in intracellular granularity are associated with cellular endpoints, such as terminal growth arrest and cell death, that are critical for the action of cancer chemotherapies, providing a useful marker to screen for novel cancer therapeutic agents. The nature of cellular changes leading to increases in intracellular granularity is dependent on the agent and cell type under investigation. For example, growth arrest associated with increases in intracellular granularity may be produced by agents that induce cellular differentiation as observed with corticotropin-releasing hormone-induced keratinocyte differentiation.⁶ Growth arrest associated with increased intracellular granularity is also a significant endpoint in terminal replicative senescence,⁷ which is being exploited for breast cancer chemo-prevention with tamoxifen, vorozole, 4-(hydroxyl-phenyl)retinamide, and 9-cis-retinoic acid.⁸ Similarly, treatment of DU145 prostate cancer cells with boric acid results in increased intracellular granularity and decreased proliferation, mimicking a senescent phenotype.⁹ Cell death pathways, such as apoptosis, may also be associated with alterations in cellular granularity.¹⁰ Recently, cell death through autophagy has been promoted as a target for cancer therapeutics,¹¹ and an important facet of autophagy is the production of autophagic vacuoles.¹² The anti-estrogens tamoxifen, OH-tamoxifen, and ICI 164 384 cause extensive accumulations of autophagic vacuoles in MCF-7 cells that correlate with cell death.¹³ Similar accumulations of autophagy-associated acidic vacuoles occurring prior to cell death have been observed following exposure of breast and prostate cancer cell lines to irradiation¹⁴ and experimental chemotherapeutics.¹⁵⁻¹⁷ Thus, both irradiation and chemotherapeutic exposure are associated with increased intracellular granularity in cell lines derived from human cancers and in chemically induced rat mammary tumors. An interesting commonality associated with these studies is the epithelial derivation of the cell lines, and there is an emerging consensus that solid tumors derived from glandular epithelium are unique in their response to therapeutic intervention.¹⁸ Whereas blood cell-derived tumors often die via apoptosis following chemotherapy, adenocarcinomas are more likely to succumb to type II cell death that is associated with increased autophagy.¹⁹ These studies support the notion that high-throughput analysis of intracellular granularity in cell lines derived from epithelial-derived cancers may provide a simple and rapid screening tool for agents that exhibit favorable qualities as cancer therapeutic agents.

Numerous human prostate cancer cell lines have been characterized²⁰ that could be useful for high-throughput phenotypic screening of small molecules. These include the extensively characterized androgen-sensitive LNCaP human prostate cancer cell line²¹ as well as the androgen-independent PC3 human prostate cancer cell line.²² The LNCaP cell line was derived from a prostate cancer lymph node metastasis,²¹ and these cells are stimulated by androgens to modulate their proliferative activity.^{21,23} Androgen receptor activation in LNCaP cells occurs from a number of ligands,²⁴ which may be the result of a mutation in the ligand-binding domain of the androgen receptor.²⁵ We have observed a change in the LNCaP cellular differentiation state and an increase in intracellular granularity after exposure to high, physiological concentrations of androgen.^{23,26} In contrast, PC3 cells were derived from a bone metastasis, and androgen treatment is not known to affect their proliferative or secretory functions.²² For the purposes of this study, both the LNCaP and PC3 human prostate cancer cell lines were used to develop high-throughput flow cytometry screens for small molecules that induce intracellular granularity because both cell lines exhibit increased accumulations of vesicles following exposure to potential chemical therapeutics.^{16,17}

Modern drug discovery strategies involve high-throughput screening (HTS), where libraries of chemical compounds are tested against a battery of relevant cell and molecular targets. Flow cytometry is an inherently high-content methodology capable of simultaneous analysis of multiple markers associated with physiological and biochemical cellular responses. HyperCyt[®] (IntelliCyt, Albuquerque, NM) is a recently developed high-throughput flow cytometry (HTFC) system, where individual microplate wells are sampled and acquired in a time-resolved manner; sample volumes of 1 to 2 μL per well are typical. This allows for the efficient utilization of scarce reagents while maintaining accurate quantitative measurements. This system has been validated using cell-based, high-throughput endpoint assays for ligand binding, surface antigen expression, and immunophenotyping.^{27,28} Here we report modifications to the LNCaP assay that make it amenable to HyperCyt[®] HTFC. Miniaturization was demonstrated by a successful screening of a collection of off-patent, marketed drugs with known safety and bioavailability in humans. This was followed by a screening of an early iteration of the National Institutes of Health Molecular Libraries Small Molecule Repository (NIH MLSMR) that contained approximately 25,000 compounds. Small molecules that significantly increased intracellular granularity in both androgen-sensitive and androgen-insensitive human prostate cancer cells in a dose-dependent manner were identified, offering useful tools for the evaluation of granularity induction in prostate cancer cells.

MATERIALS AND METHODS

Cell culture and reagents

Cell culture reagents were obtained from Invitrogen (Carlsbad, CA). Disposable tissue culture plasticware was from Griener (Monroe, NC). DMSO, dextran, and activated charcoal were obtained from Sigma (St. Louis, MO). Phosphate buffered saline (PBS) was from Mediatech Inc. (Manassas, VA). The LNCaP and PC3 human prostate cancer cell lines were obtained from the American Type Culture Collection (Manassas, VA). Cultures were kept in a humidified, 5% CO₂ atmosphere and were maintained in DMEM/low glucose, supplemented with 5% heat-inactivated FBS, 1000 U/mL penicillin, 1 mg/mL streptomycin, 25 $\mu\text{g}/\text{mL}$ amphotericin-B, and 4 mM L-glutamine. Culture medium used during screening contained 4% charcoal-stripped FBS and 1% whole FBS (DMEM/CSS). The steroid R1881 (methyltrienolone) was from PerkinElmer/New England Nuclear Life Science Products (Boston, MA), and stock solutions in DMSO (5 mM) were kept at -20°C . Two molecular libraries were screened. The Prestwick Chemical Library (Illkirch, France) is a broad spectrum collection of 880 compounds that includes numerous off-patent, marketed drugs

with known safety and bioavailability in humans. The NIH MLSMR was curated by BioFocus/DPI (South San Francisco, CA) and contains 24,718 structurally diverse compounds. Stock solutions of each library were solubilized in DMSO at 2 mg/mL and 10 mM, respectively. Charcoal-stripped FBS was prepared by mixing 0.1 g dextran and 1 g of activated charcoal with 100 mL of heat-inactivated FBS for 30 minutes at 4°C. The FBS was collected by centrifugation (8000g, 15 minutes), and the procedure was repeated before sterile filtration through a 0.22- μ m filter.

Granularity assay

Increased granularity in LNCaP cells was induced with the synthetic androgen R1881. A total of 7.5×10^5 LNCaP cells were resuspended in DMEM/CSS, placed into T-25 tissue culture flasks overnight, and were then either untreated, treated with 10 nM R1881, or treated with 1% DMSO (vehicle control). Four days after exposure to R1881, media were removed; the monolayer was rinsed with PBS, after which the LNCaP cells were exposed to a 0.05% Trypsin/EDTA solution. Cells were then collected, washed by centrifugation, and resuspended in medium, and the light scatter properties of the harvested populations were assessed by flow cytometry using a Beckman Coulter Cyan-ADP cytometer equipped with a 488-nM laser (Fort Collins, CO). Untreated populations were used to set an analysis gate for viable cells. Dose-response validation was performed in 24-well tissue culture plates as follows: LNCaP cells were resuspended in DMEM/CSS (5×10^4 /mL) and seeded at 1.5 mL per well. Following overnight incubation, a range of R1881 concentrations was added to individual wells. Negative controls consisted of no treatment or vehicle treatment with 1% DMSO. The LNCaP cells were harvested, collected, and analyzed as described above.

High-throughput screening

The LNCaP cells were resuspended in DMEM/CSS (1×10^5 /mL), and 99 μ L was added to a 384-well microtiter plate. Following overnight incubation, library compounds and controls were added as follows: column 1, cells incubated with 1% DMSO (vehicle control); column 2, medium alone; columns 3 to 22, cells incubated with library compounds; column 23, cells incubated with 10 nM R1881 (positive control); and column 24, medium alone. Compound plates were sampled (i.e., 1 μ L) using a Biomek NX/MC liquid handling system (Beckman Coulter Inc., Fullerton, CA). This resulted in a final concentration of 2 μ g/mL for the Prestwick Chemical Library and 10 μ M for the NIH MLSMR. Assay plates were harvested on day 4 as follows: medium was wicked away, 30 μ L of 0.25% Trypsin/EDTA was added, and the plates were mixed and incubated at 37°C for 15 minutes. Trypsinization was terminated by adding 10 μ L of PBS containing 20% FBS. Individual wells were immediately sampled using the HyperCyt[®] HTFC platform. The androgen-induced response range was defined by replicate control wells containing 10 nM R1881 or 1% DMSO. Signal to noise (S/N), signal to background (S/B), and Z' values were calculated as described in Zhang et al.²⁹ Assays using PC3 cells were performed as described above except that PC3 cells were seeded at 7500 cells per well. Compounds selected from the NIH MLSMR for dose-response analysis were tested in quadruplicate. Compounds were serially diluted 1:3 six times starting at 30 μ M, resulting in a concentration range of 30 μ M to 41.2 nM. The resultant data points were fitted by Prism[®] software (GraphPad Software Inc., San Diego, CA) using nonlinear least-squares regression in a sigmoidal dose-response model with variable slope, also known as the 4-parameter logistic equation. Curve fit statistics were used to determine the concentration of test compound that resulted in 50% of the maximal effect (EC₅₀), the confidence interval of the EC₅₀ estimate, the Hill slope, and the correlation coefficient.

HyperCyt[®] high-throughput flow cytometry

The HyperCyt[®] system interfaces a flow cytometer and an autosampler. While the sampling probe moves from well to well, a peristaltic pump sequentially aspirates a small volume from each well. A bubble of air, created by the continuously running pump, separates samples collected from individual wells. The air bubble-separated samples are delivered to a cytometer, and the data accumulate as a single, time-resolved file with divisions corresponding to the bubbles of air. The acquired flow cytometry data file, including time, forward light scatter, and side light scatter, is partially analyzed with specialized software that divides the data stream into 384 separate clusters. Individual data clusters are delineated by rectangular bins. Data from replicate negative control wells are pooled and used to set a split gate that defines granularity in vehicle-treated cells as a population where 10% of the cells exhibit increased granularity. This gate is used to evaluate each data cluster, and these values are automatically exported to a Microsoft Excel (Redmond, WA) spreadsheet template that tabulates the positive percentage side scatter (SSC) corresponding to individual wells.

RESULTS

R1881 increases granularity of LNCaP cells

Increased intracellular granularity of LNCaP cells after exposure to the synthetic androgen R1881 was measured by flow cytometry as shown in Figure 1. Overnight cultures of LNCaP cells were treated with 1% DMSO or R1881. After 4 days in culture, cells were collected by trypsinization, and their light-scattering properties were examined. Forward light scatter (FSC) versus side light scatter (SSC) dot plots are shown in Figure 1A and 1B. Vehicle-treated LNCaP cultures (Fig. 1A) exhibited a median SSC value of 18,165, whereas the median SSC of cultures treated with 10 nM R1881 increased to 28,900 (Fig. 1B). Another way to assess these data is to measure the percentage of cells in the treated populations with increased SSC. For this measurement, SSC is plotted as a function of cell number (event count), and a split gate is set that defines the negative control population as one in which 10% of the cells exhibit increased SSC (Fig. 1C). When this gate was applied to R1881-treated populations, the percentage of cells that exhibited increased SSC was 39.8% (Fig. 1D).

Dose-response analyses were performed to more specifically characterize the magnitude and range of this response. Overnight cultures of LNCaP cells (75,000/well) were incubated with 1% DMSO or with R1881 concentrations ranging from 1 pM to 10 nM before harvesting and evaluation by flow cytometry. A graphical representation of the collected data is shown in Figure 2. As expected, increasing concentrations of R1881 resulted in an increased percentage of LNCaP cells exhibiting increased SSC. Moreover, a time course study, where R1881-treated cells were harvested on days 2, 3, and 4, determined that the maximal percent SSC developed after 4 days of exposure to androgen (data not shown). The median SSC of treated LNCaP populations ranged from 16,059 when cells were exposed to 1 pM of R1881 to 23,558 when exposed to 10 nM R1881. The median SSC value when LNCaP populations were exposed to 1% DMSO was 14,005. When the SSC gate of the DMSO control was set at 10%, the percentage of SSC positive of the treated populations ranged from 13.5% in the presence of 1 pM R1881 to 37.6% in the presence of 10 nM R1881. The calculated EC₅₀s for these data were 514 pM (median SSC v. R1881) and 122 pM (% SSC positive v. R1881) of R1881, respectively.

HyperCyt[®] high-throughput flow cytometry

The relative ease of flow cytometry, where 10,000 cells can be analyzed in seconds, offers a quantitative approach for screening compound libraries. Not unexpectedly, developing a

miniaturized, flow cytometry-based, high-throughput assay from the model system described above presented challenges, the first being the adherent property of LNCaP cells. Previous studies with the HyperCyt[®] platform used analyte-bound, microfluidic beads²⁷ or suspension cultures²⁸ set up in 96- and 384-well microtiter plates, neither of which required trypsinization. Flask cultures of prostate cancer cells are typically passaged with a 0.05% trypsin solution; however, this concentration proved unworkable in this homogeneous, no-wash, 384-well system because it resulted in clumps of LNCaP cells that regularly clogged the autosampler tubing, leading to unacceptably low event counts per well. A range of cell numbers per well (2000–20,000) and trypsin conditions (10–30 μ L of 0.25% trypsin; 5–15 minutes at 37°C) were tested before a standard treatment protocol was achieved (30 μ L of 0.25% trypsin; 15 minutes at 37°C). When a 384-well microtiter plate was seeded with 10,000 cells per well and incubated for 5 days, an event count where column averages ranged from 503 to 783 events per well was observed during sampling (1.2 s/sip). Of the 352 wells that contained cells, only 3 samplings resulted in an event count of less than 100, and there were no wells where less than 30 cells were sampled. During HTS, wells where less than 30 events were recorded were labeled “missing” and were flagged by the analysis program. Cell carryover from well to well was assessed in columns 2 and 24 where no cells were seeded. These wells contained approximately 7% of the previous well contents. For example, an event count of 813 from column 1 was followed by an event count of 53 from column 2 where no cells were seeded.

Dose-response analyses were used to validate the miniaturized, plate-based assay. A representative experiment is shown in Figures 3 and 4. Replicate ($n = 8$) microplate wells containing 10,000 LNCaP cells were exposed to 2-fold serial dilutions of R1881 ranging from 100 nM to 0.4 pM. Figure 3A and 3B show the single-file data stream as a scatter plot and a histogram, respectively. The 384 time-resolved data clusters acquired during the 1.2-second samplings are shown in Figure 3C, and one row of sampled wells is shown in Figure 3D. Negative control wells ($n = 8$) were selected and displayed (Fig. 3E), and a split gate was set at 10% (Fig. 3F). This gate was then applied to individual sample wells containing the varying concentrations of R1881. One dose-response set of treated samples is displayed in Figure 3G. Data from replicate samples were then used to construct the dose-response curve seen in Figure 4. The calculated EC₅₀ was somewhat higher than that observed for the “bulk” analysis shown in Figure 2 (182 pM v. 122 pM).

Prestwick Chemical Library Screening

The Prestwick Chemical Library is comprised of 880 high-purity small molecules of which 85% are off-patent drugs. These include a number of steroids and alkaloids that cover a broad range of therapeutic uses. The Prestwick Library was screened at a final concentration ranging from 2 to 10 μ M (1:1000 dilutions of compound stocks). The LNCaP cells were placed in columns 1 and 3 to 23 of a 384-well microtiter plate at 10,000 cells per well. Cells in column 1 were exposed to 1% DMSO, cells in columns 3 to 22 were exposed to test compounds, and cells in column 23 were exposed to 10 nM R1881; columns 2 and 24 did not contain cells and bracketed the negative control column. This pattern was chosen to limit the carryover of cells to and from the negative control wells because data pooled from LNCaP cells treated with 1% DMSO were used as the reference to set the 10% split gate as shown in Figure 3. Thus, treatment responses are evaluated based on comparison to the negative control samples. The Prestwick Library was screened a total of 5 times, and data from a representative screen and the statistical analysis of the data are given in Table 1. Negative and positive control wells ($n = 16$) were pooled and used to calculate Z' values. One characteristic of LNCaP cells is their variable response to R1881,³⁰ and the representative data shown in Table 1 reflect this variable response where plate averages ranged from 38.1% to 53.4% SSC positive in response to 10 nM R1881. This variability is

also reflected in the relatively low S/N and S/B ratios as well as the suboptimal Z' values (see discussion of assay reliability). Phenotypic assays are inherently variable, and their use in HTS has been associated with increased false negatives and positives.^{31,32} In this instance, the Prestwick Library contains a nominal internal standard, testosterone, where a positive signal might be anticipated. In 4 of the 5 screens, exposure to testosterone resulted in a 30% SSC positive rate ($31\% \pm 3\%$). This response rate was used to define a primary screen “hit” as any compound that resulted in $>30\%$ SSC positivity. The total number of compounds identified in the Prestwick Chemical Library that satisfied this hit selection criteria was 140, corresponding to a hit rate of 16%. This hit rate is similar to a recent image-based screen of the ICCB BIOMOL library that was designed to identify positive regulators of autophagy; 15% of the 480 compounds tested were identified as hits.³³

NIH MLSMR screening

The primary screen of the NIH MLSMR was performed essentially as described above for screening LNCaP cells against the Prestwick Chemical Library. The initial screen was carried out at 10 μM . Results of the primary screen of 24,718 compounds identified 134 compounds (0.5%) that satisfied the hit selection criteria ($>30\%$ SSC positive) regarding increased LNCaP granularity. Similar to the Z' values calculated for the third Prestwick Library plate, most of the calculated Z' values approached zero. As mentioned above, the low Z' values were likely attributable to the variable response of high-passage LNCaP cells to R1881^{30,34} and it was this response that was used to define the assay’s dynamic range.

A majority of the active compounds shared a common structural motif, most often consisting of an aromatic heterocyclic moiety that was separated from a basic tertiary amine by an aliphatic amide. A portion of the 134 actives were assigned to 1 of 5 chemotype families based on substructure analysis shown in Table 2. Family 1 was clustered around the 1-[[2-phenyl-5-methyl-4-oxazolyl] methyl]-piperidinecarboxamide having both 1,3- and 1,4-substituted piperidine region-isomers (1,4-shown). The 3-phenyl-1-methyl-1H-Thieno[2,3-c]pyrazole-5-carboxamide substructure of family 2 defines a similar steric space as does family 1. Family 3 was clustered around a 2-piperazinyl-quinoline carboxamide, family 4 around a 1, 3-dialkyl, 2-aminobenzimidazole, and family 5 around a comparatively simple N-aryl piperidine subgroup. A number of the singleton actives were morphologically similar to the clustered families, but they yielded little biological or structure-activity information. These 134 compounds were selected for follow-up analysis as were 177 structurally related compounds. An additional 119 compounds were designated as “missing” based on a well event count that was less than 30. In rare instances, a “missing” well results from a mechanical sampling error. More common were those instances where a significantly reduced event count was the result of compound toxicity that either killed LNCaP cells or resulted in a loss of adherence (data not shown). Because cell death or senescence has been related to intracellular granularity,⁸⁻¹⁷ these 119 compounds were also chosen for follow-up. Another reason for expanding our initial selection was our concern regarding an increased rate of false negatives because testosterone was not reproducibly detected as an active compound.

Three additional single-point screens were performed on LNCaP cells using these 430 compounds, 1 at 100 μM and 2 at 10 μM . The results of the primary and secondary single-point screens have been deposited into the PubChem database (<http://www.ncbi.nlm.nih.gov>; AID 795, 1069, 1076). Outcome data from both the primary single-point screen and the second set of single-point screens were used to identify 95 compounds of interest: 72 designated as “actives,” and 23 designated as “missing.” These 95 compounds were tested in a dose-response format where compounds were tested in quadruplicate at 7 different concentrations ranging from 30 μM to 100 nM. In order to delineate potential androgenic from nonandrogenic responses, both LNCaP cells and PC3 cells were tested.

Compounds were considered “hits” if the estimated EC₅₀ for SSC positivity was less than 10 μM. The best responder from each of the 5 chemotype families is depicted in Table 2, and the corresponding dose-response data for these compounds are shown in Figure 5. Figure 5 also includes a composite histogram where the mean event count for the 3 highest concentrations is shown. Significantly reduced event counts were typically observed when either cell line was exposed to the 30 μM concentration.

Table 2 also provides biological activity profiles of the most active family members available from the PubChem database. A database substructure search of families 1 to 4 revealed commonalities among the activities of these families. The most common involved potential cytotoxicity measured using viability staining techniques. Families 2, 3, and 4 were similarly associated with reduced activation of a mitogen-activated kinase essential for cell growth and survival. These data complement our observations regarding event count and this assay’s endpoint of increased granularity because a significantly lowered event count is likely indicative of a compound’s toxicity and increased granularity is possibly the result of accumulations of intracellular membranous organelles associated with autophagy.^{11–17} While there were also unique activities associated with each substructure, these assays were most often counterscreens designed to exclude nonspecific compounds or chemical profiling assays that identified compound fluorescence or insolubility. The substructure search of family 5 identified over 10,000 substances limiting its utility vis-a-vis scaffold-based promiscuity profiling. Similar promiscuity searches using the best-in-class compound from each family revealed a strikingly specific profile. The best overall compound, CID 3240581 from family 1, was only confirmed as an active in this screening effort, and the only compound that demonstrated any real promiscuity, CID 5308376, from family 2, was a confirmed active in viability screens (i.e., potential toxic compound).

Each family was also evaluated on its overall activity while taking scaffold promiscuity and tractability into consideration. Families 3 and 4 were effectively dismissed from further consideration early in the confirmatory screening process. Together, these 2 families contained 23 members, and the 6 actives demonstrated limited activity when screened against PC3 cells. This pattern is exemplified by the most active family 3 compound, CID 3240925. While the EC₅₀ with PC3 cells (2.21 μM) was better than what was seen with LNCaP cells (3.45 μM), the maximal effect in PC3 cells was less than 30% (Fig. 5C). In contrast, the best active from family 4 (CID 2858099) exhibited an EC₅₀ of 0.99 μM when tested against LNCaP cells, and a 10 μM treatment of PC3 cells resulted in greater than 50% of the population exhibiting increased SSC (Fig. 5D).

Table 3 illustrates the activity of key members of families 1, 2, and 5, with their rankings dependent on their activity against LNCaP cells. The scaffold is depicted in the table header, and modifications are noted by regions 1 (R¹) and 2 (R²) that represent variability at the amine and the heterocyclic moiety, respectively. Family 1 contained the most members and most potent actives. Both 1,3- and 1,4-piperidine-substituted compounds were screened with a 1,4-substitution demonstrating greater overall activity. Although there was no obvious trend in SAR around R², 4-chloro and 2-methyl analogs predominated in the actives. While a variety of R² substituents were screened including alkyl, heteroalkyl, aryl, and heteroaryl groups, alkyl-linked tertiary amines (compounds 1–7) exhibited the best activity. The simple alkyl amines 1, 2, and 3 were the most active compounds, and compound 1 demonstrated submicromolar potency. This compound was significantly more active in LNCaP cells than PC3 cells (EC₅₀ of 768 nM v. 6.5 μM) (Fig. 5A), contrasting the activities of compounds 2 and 3. Two additional simple alkyl amines (4 and 6) were less active as was the morpholino-containing compound 5. Moderate activity was observed with 2 other morpholine analogs.

Although family 2 is represented by fewer members, its chemotype could be considered an extension of family 1. Regarding its isosteric counterparts in family 1, 4-chloro, R¹ substituents predominate in family 2 actives. Furthermore, family 2 inactives share an almost identical R² substituent profile with family 1, including alkyl, aryl, heteroaryl, carbonyl-containing, and di-substituted ring-fused groups. Although the activity is generally lower than family 1, alkyl amines in R² predominate (compounds 8–14). In contrast to family 1 actives, family 2 actives exhibited lower EC₅₀ values when tested against PC3 cells. The most active compound (CID 5308376) had an EC₅₀ of 3.35 μM against LNCaP cells and an EC₅₀ of 1.46 μM against PC3 cells (Fig. 5B). Family 5 was the most structurally varied due to the simple scaffold used for substructure clustering. Overall this is a low activity family, and compounds 15 to 18 are representative of the actives. Figure 5E shows the dose-response analysis of the most active compound, and while its EC₅₀ was below 2 μM, it exhibited the smallest maximal effect against LNCaP cells.

DISCUSSION

We have developed a phenotypic assay based on our original findings regarding androgen-induced increases in intracellular granularity in the LNCaP prostate cancer cell line²⁶ and on significant findings regarding increases in the acidic vacuolar compartment of adenocarcinoma-derived human cell lines following exposure to irradiation or novel small molecules.^{8,9,13–17} The miniaturized, 384-well microtiter plate assay was developed and optimized using the HyperCyt[®] HTFC platform. Validation consisted of a screen of the Prestwick Chemical Library that contains a number of steroids and alkaloids covering a broad therapeutic range. In 4 of 5 screens, testosterone exposure was identified as a hit, and this response (~30% SSC positive) was used to define an active response to library compounds. The Prestwick screen also identified compounds that are known to increase the accumulation of autophagic vacuoles.³³ This was followed by a screen of 24,718 small molecules that identified 134 actives corresponding to a hit rate of 0.5%. Confirmation analysis entailed a rescreening of 430 compounds, resulting in the identification of 95 compounds of interest. Dose-response analysis utilizing the HTFC platform identified aryl oxazoles as being the most active. The effects of active compounds on prostate cancer cell lines shown in Table 3 are expected to follow a predictable pattern. Increased secretory activity can be further evaluated by measuring changes in mitochondrial content and the secretion of PSA.^{23,26} Compounds that lack differentiative activity can be further assessed using standard techniques associated with an analysis of autophagy.^{33,35} These include staining treated cells with acridine orange and lysotracker green as well as by following the expression of the lysosome-associated protein LC3 II.^{15,33} There would be value in testing active compounds from the identified chemotypes on other cells lines derived from both epithelial and nonepithelial cancers where these compounds could serve as chemical probes for pathway analysis of intracellular granularity leading to the development of novel strategies for prostate cancer therapy. Experiments following resynthesis of compound 3240581 confirmed our results with the MLSMR-derived compound regarding granularity induction in LNCaP and PC3 cells.

Assay reliability

The Z' value is a measure of screening assay quality that reflects both the dynamic range of an assay as well as an assay's data variation. Zhang et al. defined excellent assays as those where the Z' value was greater than 0.5.²⁹ Assays where the Z' value approached zero were termed yes/no assays. Cell-based, phenotypic assays such as the one described here present a particular problem for Z' calculations because they often have a narrow dynamic range and are inherently variable due to cellular heterogeneity and the complex nature of phenotypic responses that involve multiple interacting molecular pathways.^{31,32} These caveats are

reflected by the relatively low S/N and S/B ratios as well as by the suboptimal Z' values shown in Table 1. This is especially true for the third plate of the Prestwick Library, where a negative Z' value was calculated due a response to R1881 that ranged from 15% to 54% SSC positive. Variable responses of LNCaP cells have been reported previously; genetic heterogeneity of the parental LNCaP cell line is thought to cause increased resistance to growth inhibition and the concomitant promotion of secretory functions induced by 10 nM R1881, and it is possible that the variable response seen here reflects this genetic heterogeneity.^{30,34}

That being the case, the Prestwick Chemical Library, because it contains testosterone as well as other steroids with potential androgenic activity, offered a useful test case. We reasoned that the utility of this assay would be reflected by its ability to detect increased granularity following treatment of LNCaP cells with testosterone, a compound with well-characterized activity. We screened LNCaP cells on 5 separate occasions, and in 4 of the 5 screens, testosterone exposure resulted in a ~30% SSC positive ($31\% \pm 3\%$). Exposure to the steroidal compounds ethisterone and nor-ethisterone, 17 α -ethynyl analogs of testosterone, resulted in average SSC positive populations of $59.5\% \pm 9.8\%$ and $34\% \pm 14\%$, respectively. The LNCaP cells carry a point mutation in the ligand-binding domain of the androgen receptor that affects steroid-binding characteristics leading to enhanced affinity for, and activation by, estrogenic and progestogenic steroids,^{24,25} which may explain the observed response to the 17 α -ethynyl analogs of testosterone as both are known ligands for estrogen and progesterone receptors. This contrasted with a single screen using the androgen nonresponsive PC3 prostate cancer cells where the SSC positive populations were 15%, 10%, and 10%, following exposure to testosterone, ethisterone, and nor-ethisterone, respectively. With regards to false negatives, while the responses of LNCaP cells to testosterone analogs could not have been predicted, a response to testosterone was anticipated, and these data support the notion that this phenotypic assay may be prone to false-negative identification.

A second test case was offered by other small molecules contained in the Prestwick Library. As mentioned above, tamoxifen induces the accumulation of autophagic vacuoles in MCF-7 cells,¹³ and tamoxifen as well as 2 other compounds from the Prestwick Library, namely trifluoperazine and amio-darone, have recently been identified as regulators of autophagy due to their ability to increase the extent and localization of the microtubule-associated protein LC3 to intracellular autophagic vacuoles.³³ All 3 compounds induced positive SSC populations in LNCaP cells with averages that ranged from 32% for tamoxifen to 56% for trifluoperazine. However, in each instance, there was a sample value that did not achieve the hit rate of 30%, again confirming our experience regarding false negatives. Trifluoperazine was the most potent inducer of the 3 compounds. In 3 of the 5 screens, trifluoperazine induced a SSC positive population that exceeded 60%, and a similar screen using PC3 cells resulted in SSC positivity of 64%. When a dose-response analysis of trifluoperazine was performed on LNCaP cells, we observed an EC_{50} of 3.3 μ M (data not shown). These data strongly suggested that the HTS assay could accurately detect increased granularity in LNCaP cells after exposure to androgens and in both responsive and nonresponsive prostate cell lines after exposure to positive regulators of autophagy that modulate intracellular autophagosomes.³³

Two additional considerations regarding assay performance deserve attention. The first is the issue of low event counts. While our initial studies indicated that a sufficient number of cells were sampled at 1.2 s/sip, these studies did not consider potential toxic effects of compounds that could result in reduced cell counts. In fact, any compound effect that results in a cell becoming nonadherent would reduce the number of events because medium is removed before trypsin treatment and non-adherent cells would be lost during this step.

Therefore, wells where less than 30 events were sampled were scored as “missing,” and the compounds were considered potentially toxic. Secondly, as mentioned above, a select group of nonsteroidal compounds consistently resulted in increased granularity in both LNCaP and PC3 cells. Because the biomolecular pathways that result in granularity are not exclusive to the increases observed when LNCaP cells are stimulated with androgens,²⁶ whether these nonsteroidal compounds act on other cellular processes that affect granularity is unknown. For instance, increased mitochondria would necessarily result in increased granularity, and as mentioned above, cellular senescence,^{7–9} terminal differentiation,⁶ and autophagy^{11–17} have been associated with increases in granularity.

In retrospect, based on the variable response of LNCaP cells to R1881 over time, it might have made sense to seek an alternate positive control for the MLSMR screen, which would have meant restarting the screen. Unfortunately, when the positive control failed altogether, the Z' scores for some plates were considerably below zero, even though the negative control was highly reproducible. However, when the Prestwick screen was performed on the PC3 cells, which were more readily resuspended, and using metergoline as a positive control, the 3 plates yielded Z' scores of 0.5, 0.28, and 0.05, respectively. Thus, while the Z' values for individual plates were suboptimal in the initial LNCaP screen, we were confident that by rescreening individual compounds and related family members as well as questionable plates (31/88) and missing wells against both LNCaP and PC3 targets, we would identify active compounds. Moreover, the improvement in assay performance for the PC3 cells suggests that the approach can be extended to other cell lines.

Acknowledgments

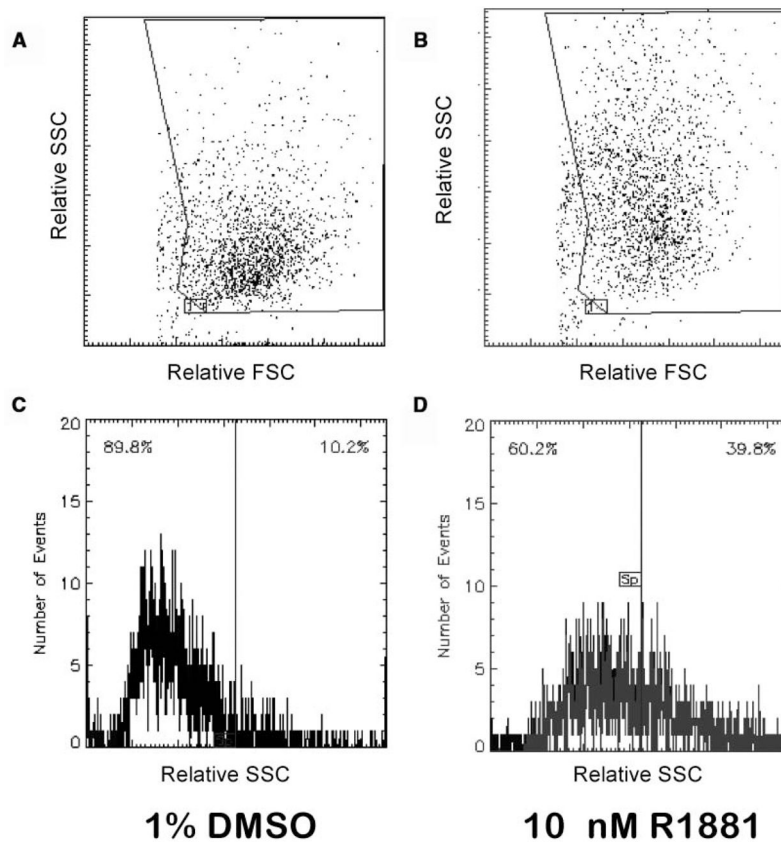
This research was supported by grants NIH 1 X01 MH 078937-01 to TAT and NIH U54 MH074425-01 to the New Mexico Molecular Libraries Screening Center, NIH U54 MH084690 to the University of New Mexico Center for Molecular Discovery, the University of New Mexico Shared Flow Cytometry Resource (CA 118100, Cheryl L. Willman, MD), the UNM tobacco settlement, and the UNM Cancer Center. The authors thank Mark B. Carter, MSc, and Susan A. Young, MSc, for the flow cytometry expertise and Debra A. MacKenzie, PhD, and Virginia M. Salas, PhD, for their critical review of the article.

References

1. Jemal A, Siegel R, Ward E, Hao Y, Xu J, Murray T, Thun MJ. Cancer statistics, 2008. *CA Cancer J Clin.* 2008; 58:71–96. [PubMed: 18287387]
2. Burton JL, Oakley N, Anderson JB. Recent advances in the histopathology and molecular biology of prostate cancer. *BJU Int.* 2000; 85:87–94. [PubMed: 10619953]
3. D'Amico AV, Whittington R, Malkowicz SB, Fondurulia J, Chen MH, Kaplan I, et al. Pretreatment nomogram for prostate-specific antigen recurrence after radical prostatectomy or external-beam radiation therapy for clinically localized prostate cancer. *J Clin Oncol.* 1999; 17:168–172. [PubMed: 10458230]
4. Steineck G, Helgesen F, Adolphsson J, Dickman PW, Johansson JE, Norlén BJ, Holmberg L. Quality of life after radical prostatectomy or watchful waiting. *N Engl J Med.* 2002; 347:790–796. [PubMed: 12226149]
5. Ip C, Hall SJ. Hormonal implications in the development and treatment of prostate cancer. *Endocrinol Metab Clin N AM.* 2007; 36:421–434.
6. Zbytek B, Pikula M, Slominski RM, Mysliwski A, Wei E, Wortsman J, Slominski AT. Corticotropin-releasing hormone triggers differentiation in HaCaT keratinocytes. *Br J Dermatol.* 2005; 152:474–480. [PubMed: 15787816]
7. Sherwood SW, Rush D, Elsworth JL, Schimke RT. Defining cellular senescence in IMR-90 cells: a flow cytometric analysis. *Proc Natl Acad Sci.* 1985; 85:9086–9090. [PubMed: 3194411]
8. Christov KT, Shilkaitis AL, Kim ES, Steele VE, Lubet RA. Chemopreventive agents induce a senescence-like phenotype in rat mammary tumours. *European J Cancer.* 2003; 39:230–239. [PubMed: 12509956]

9. Barranco WT, Eckhart CD. Cellular changes in boric acid-treated DU-145 prostate cancer cells. *Br J Cancer*. 2006; 94:884–890. [PubMed: 16495920]
10. Dive C, Gregory CD, Phipps DJ, Evans DL, Milner AE, Wyllie AH. Analysis and discrimination of necrosis and apoptosis (programmed cell death) by multiparameter flow cytometry. *Biochim Biophys Acta*. 1992; 1133:275–285. [PubMed: 1737061]
11. Rubinsztein DC, Gestwicki JE, Murphy LO, Klionsky DJ. Potential therapeutic applications of autophagy. *Nat Rev Drug Disc*. 2007; 6:304–312.
12. Monastyrska I, Klionsky DJ. Autophagy in organelle homeostasis: peroxisome turnover. *Mol Aspects Med*. 2006; 27:483–494. [PubMed: 16973210]
13. Bursch W, Ellinger A, Kienzl H, Török L, Pandey S, Sikorska M, et al. Active cell death induced by the anti-estrogens tamoxifen and ICI 164384 in human mammary carcinoma cells (MCF-7) in culture: the role of autophagy. *Carcinogenesis*. 1996; 17:1595–1607. [PubMed: 8761415]
14. Paglin S, Hollister T, Delohery T, Hackett N, MacMahill M, Sphicas E, et al. A novel response of cancer cells to radiation involves autophagy and formation of acidic vesicles. *Cancer Res*. 2001; 61:439–444. [PubMed: 11212227]
15. Arthur CA, Gupton JT, Kellogg GE, Yeudall WA, Cabot MC, Newsham IF, Gewirtz DA. Autophagic cell death, polyploidy and senescence induced in breast tumor cells by the substituted pyrrole JG-03-14, a novel microtubule poison. *Biochem Pharm*. 2007; 74:981–991. [PubMed: 17692290]
16. Suárez Y, González L, Cuadrado A, Berciano M, Lafarga M, Muñoz A, Kahalalide F, a new marine-derived compound, induces oncosis in human prostate and breast cancer cells. *Mol Cancer Ther*. 2003; 2:863–872. [PubMed: 14555705]
17. Wang M, Tan W, Zhou J, Leow J, Go M, Lee HS, Casey PJ. A small molecule inhibitor of isoprenylcysteine carboxymethyltransferase induces autophagic cell death in PC3 prostate cancer cells. *J Biol Chem*. 2008; 283:18678–18684. [PubMed: 18434300]
18. Finkel E. Does cancer therapy trigger cell suicide? *Science*. 1999; 286:2256–2258. [PubMed: 10636781]
19. Zakeri Z, Bursch W, Tenniswood M, Lockshin RA. Cell death: programmed apoptosis, necrosis or other? *Cell Death Differ*. 1995; 2:87–96. [PubMed: 17180070]
20. Webber MM, Bello D, Quader S. Immortalized and tumorigenic adult human prostatic epithelial lines: characteristics and applications. Part 2: tumorigenic cell lines. *Prostate*. 1997; 30:58–64. [PubMed: 9018337]
21. Horoszewicz JS, Leong SS, Kawinski E, Karr JP, Rosenthal H, Chu TM, et al. LNCaP model of human prostatic carcinoma. *Cancer Res*. 1983; 43:1809–1818. [PubMed: 6831420]
22. Kaighn ME, Narayan KS, Ohnuki Y, Lechner JF, Jones LW. Establishment and characterization of a human prostatic carcinoma cell line (PC-3). *Invest Urol*. 1979; 17:16–23. [PubMed: 447482]
23. Bauer JA, Thompson TA, Church DR, Ariazi EA, Wilding G. Growth inhibition and differentiation in human prostate cancer cells induced by the vitamin D analog 1-alpha,24-dihydroxy vitamin D2. *Prostate*. 2003; 55:159–167. [PubMed: 12692781]
24. Wilding G, Chen M, Gelmann EP. Aberrant response in vitro of hormone-responsive prostate cancer cells to antiandrogens. *Prostate*. 1989; 14:103–115. [PubMed: 2710689]
25. Veldscholte J, Berrevoets CA, Ris-Stalpers C, Kuiper GG, Jenster G, Trapman J, et al. The androgen receptor in LNCaP cells contains a mutation in the ligand binding domain which affects steroid binding characteristics and response to antiandrogens. *J Steroid Biochem Mol Biol*. 1992; 41:665–669. [PubMed: 1562539]
26. Thompson TA, Church DR, Zhong W, Oberly TD, Wilding G. Terminal differentiation induction in LNCaP human prostate cancer cells. *Proc Am Assoc Cancer Res*. 2004; 45:889.
27. Kuckuck FW, Edwards BS, Sklar LA. High throughput flow cytometry. *Cytometry*. 2001; 44:83–90. [PubMed: 11309812]
28. Young SM, Bologa C, Prossnitz ER, Oprea TI, Sklar LA, Edwards BS. High-throughput screening with HyperCyt[®] flow cytometry to detect small molecule formylpeptide receptor ligands. *J Biomol Screening*. 2005; 10:374–382.
29. Zhang J-H, Chung TDY, Oldenburg KR. A simple statistical parameter for use in evaluation and validation of high throughput assays. *J Biomol Screen*. 1999; 4:67–73. [PubMed: 10838414]

30. Esquenet M, Swinnen JV, Heyns W, Verhoeven G. LNCaP prostatic adenocarcinomas cells derived from low and high passage numbers display divergent responses not only to androgens but also to retinoids. *J Steroid Biochem Mol Biol.* 1997; 62:391–399. [PubMed: 9449242]
31. Titus S, Neumann S, Zheng W, Southall N, Michael S, Klumpp C, et al. Quantitative high-throughput screening using a live-cell cAMP assay identifies small-molecule agonists of the TSH receptor. *J Biomol Screen.* 2008; 13:120–127. [PubMed: 18216391]
32. Chung N, Zhang XD, Kreamer A, Locco L, Kuan PF, Bartz S, et al. Median absolute deviation to improve hit selection for genome-scale RNAi screens. *J Biomol Screen.* 2008; 13:149–158. [PubMed: 18216396]
33. Zhang L, Yu J, Pan H, Hu P, Hao Y, Cai W, et al. Small molecule regulators of autophagy identified by an image-based high-throughput screen. *PNAS.* 2007; 104:19023–19028. [PubMed: 18024584]
34. Van Steenbrugge GJ, Van Uffelen CJC, Bolt J, Schroder FH. The human prostatic cancer cell line LNCaP and its derived sublines: an in vitro model for the study of androgen sensitivity. *J Steroid Biochem Mol Biol.* 1991; 40:207–214. [PubMed: 1958522]
35. Klionsky DJ, Cuerva AM, Seglen PO. Methods for monitoring autophagy from yeast to human. *Autophagy.* 2007; 3:181–206. [PubMed: 17224625]

**FIG. 1.**

The synthetic androgen R1881 causes increased intracellular granularity in LNCaP cells. Flask cultures of LNCaP cells were treated with 10 nM R1881 or 1% DMSO for 4 days followed by flow cytometric analysis. Plots of forward light scatter (FSC) versus side light scatter (SSC) (**A**, **B**) and SSC versus cell number (**C**, **D**) is shown. The 10 nM R1881 treatment (**B**, **D**) increased the mean SSC of the LNCaP population (28,900 v. 18,165) as well as the number of cells that exhibited increased SSC (10.2% v. 39.8%) when compared to 1% DMSO (**A**, **C**).

LNCaP R1881 Dose response

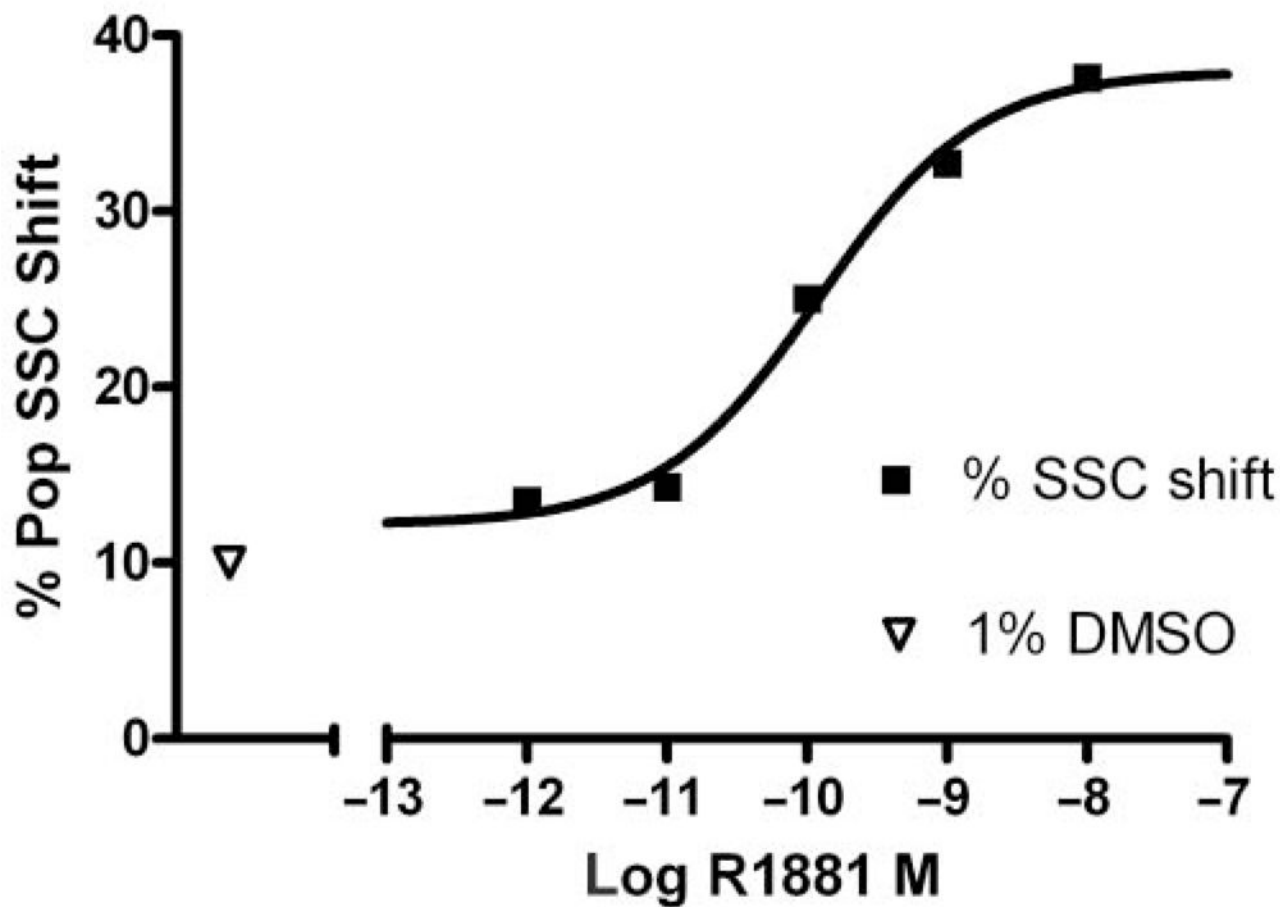


FIG. 2. Concentration response of LNCaP cells to R1881 treatment. A total of 75,000 cells per well were incubated for 4 days with 1% DMSO or varying concentrations of R1881 followed by flow cytometric analysis. The R1881 EC₅₀ was 122 pM. SSC, side scatter.

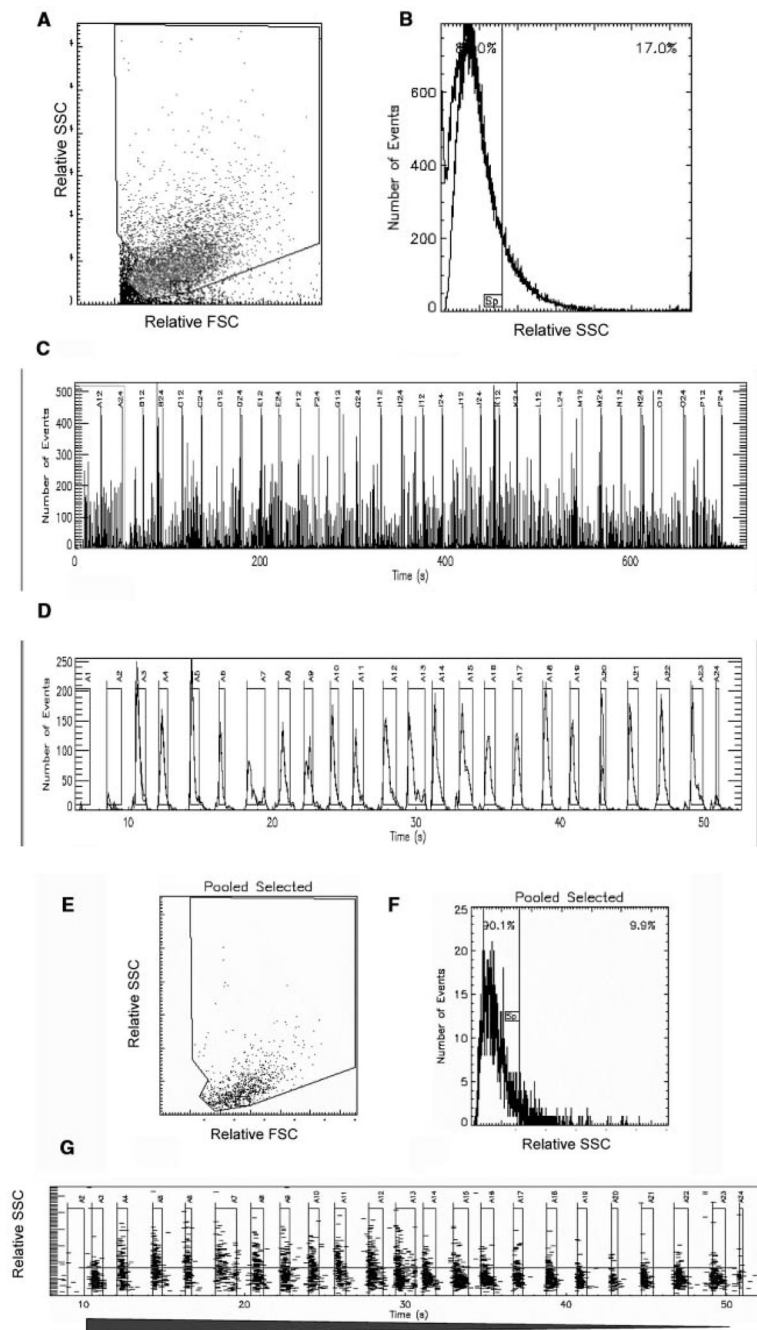


FIG. 3. HyperCyt[®] high-throughput flow cytometry. Individual wells of a 384-well microtiter plate were seeded at 10,000 LNCaP cells per well. Following overnight incubation, 2-fold serial dilutions of R1881 in DMSO were added to replicate wells ($n = 8$). Negative control wells ($n = 8$) contained 1% DMSO. Plots of forward light scatter (FSC) versus side light scatter (SSC) (**A**) and SSC versus cell number (**B**) represent the entire data set as a single file. The time-resolved format of the entire data set and one dose-response set of “binned” sample wells are shown in **C** and **D**, respectively. Pooled negative control samples (**E**, **F**) are used to set a 10% SSC split gate that is applied to the treated samples; the “binned” set shown in **D**

is represented in **G**, where decreasing concentrations of R1881 (filled arrow) result in a decreased percentage of LNCaP cells exhibiting heightened SSC.

HyperCyt R1881 Titration

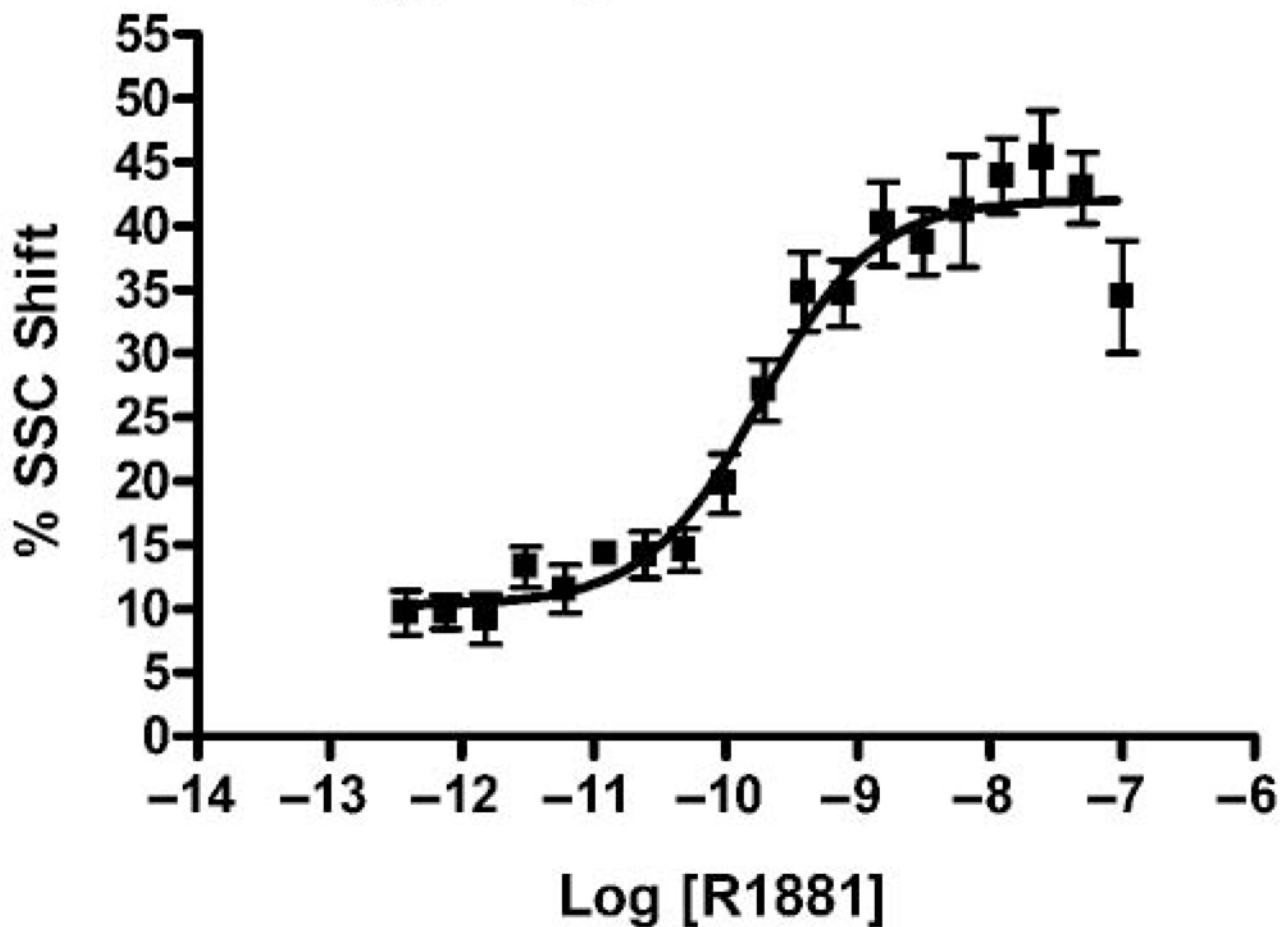


FIG. 4. HyperCyt[®] analysis of the concentration response of LNCaP cells to R1881. Individual wells of a 384-well microtiter plate were seeded at 10,000 LNCaP cells per well. Following overnight incubation, 2-fold serial dilutions of R1881 in DMSO were added to replicate wells ($n = 8$). Negative control wells ($n = 8$) contained 1% DMSO. The R1881 EC_{50} was 182 pM. SSC, side scatter.

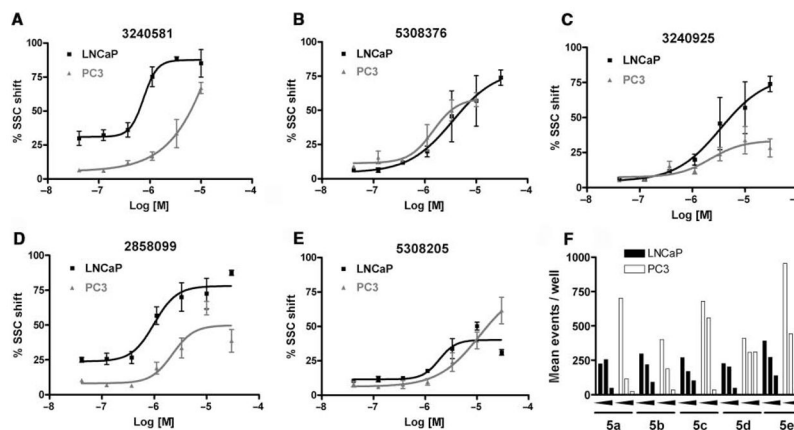


FIG. 5. Dose-response curves of the best representative compounds from the 5 families discussed in Table 2. LNCaP (closed squares); PC3 (closed triangles). Methods were essentially as described for Figure 4 except that PC3 cells were seeded at 7500 cells per well. (A) LNCaP EC_{50} was $0.77 \mu\text{M}$, and PC-3 EC_{50} was $6.5 \mu\text{M}$. (B) LNCaP EC_{50} was $3.35 \mu\text{M}$, and PC3 EC_{50} was $1.46 \mu\text{M}$. (C) LNCaP EC_{50} was $3.45 \mu\text{M}$, and PC3 EC_{50} was $2.21 \mu\text{M}$. (D) LNCaP EC_{50} was $0.99 \mu\text{M}$, and PC-3 EC_{50} was $2.21 \mu\text{M}$. (E) LNCaP EC_{50} was $1.87 \mu\text{M}$, and PC3 EC_{50} was $11.14 \mu\text{M}$. (F) A composite graph indicating the event count observed when the cells were exposed to 3, 10, and 30 μM of the 5 compounds depicted in the graphs.

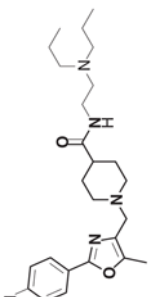
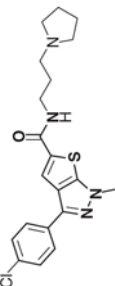
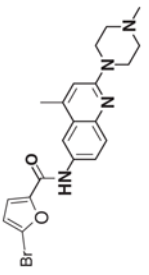
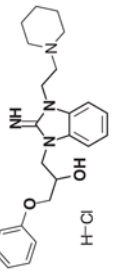
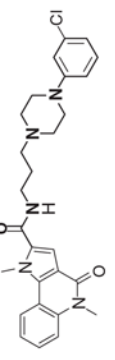
Table 1

Statistical Analysis of the Single-Point Screen of the Prestwick Chemical Library

	PCL Plate 1	PCL Plate 2	PCL Plate 3
Mean % SSC positive NC \pm SD	9.2 \pm 2.3	10.2 \pm 5.1	10.3 \pm 3.4
Mean % SSC positive PC \pm SD	39.1 \pm 6.3	53.4 \pm 7.3	38.1 \pm 12.2
S/N, S/B	13.0, 4.3	8.5, 5.2	8.2, 3.7
Z'	0.13	0.14	-0.68

The Prestwick Chemical Library (PCL) was screened as described in the Materials and Methods section using LNCaP human prostate cancer cells. SSC, side light scatter; NC, pooled negative control; PC, pooled positive control; SD, standard deviation; S/N, signal to noise ratio (PC mean – NC mean/NC SD); S/B, signal to background ratio (PC mean/NC mean); $Z' = 1 - (3SD\ PC + 3SD\ NC)/(PC\ mean - NC\ mean)$. Mean % SSC was derived as follows: data from replicate negative control wells were pooled and were used to set a split gate that defined base-line granularity in DMSO-treated cells as a population where 10% of the cells exhibit increased granularity. This gate was applied to all of the treated samples.

Table 2
Activity Profile of Identified Chemotype Substructures from the Primary MLSMR Screen

Family	LNCaP Screen ^d		LNCaP Best in Class ^b		EC ₅₀ (μM)	PubChem Activity Profile ^c	
	Tested	Active	Structure	Tested		Active	Confirmatory
1	78	18		238	0.77	13	3 (3)
2	50	7		237	3.35	23	9 (1)
3	15	3		211	2.79	14	5 (3)
4	8	3		239	0.99	9	2 (2)
5	60	10		214	1.87	14	4 (2)

LNCaP, lymph node cancer of the prostate human cell line; EC₅₀, half maximal effective concentration; CID, PubChem compound identification number; AID, PubChem assay identification number.

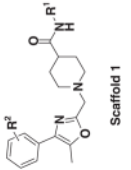
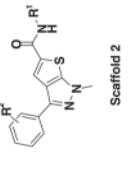
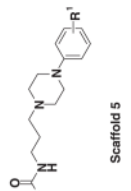

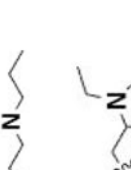
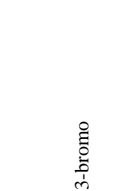
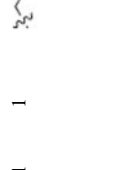
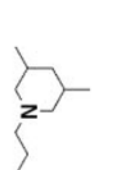


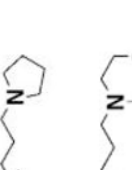
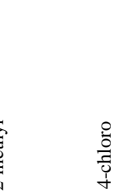

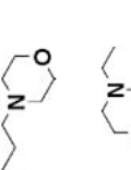
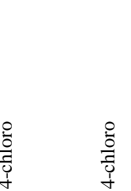
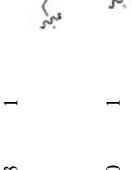
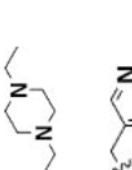
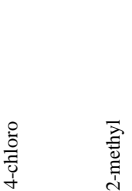

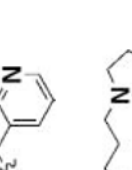
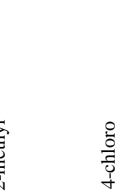
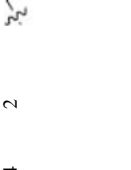
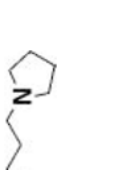

^aThe number of compounds from each family tested and found active in the primary high-throughput screen (AID #795). Compounds with EC₅₀ values <30 μM were considered active.

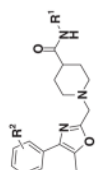
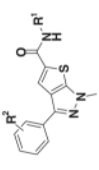
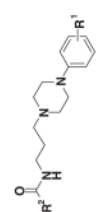
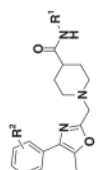
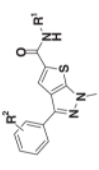
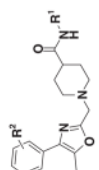
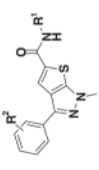
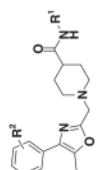
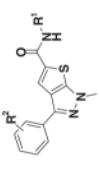
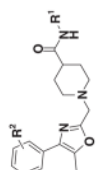
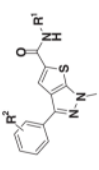
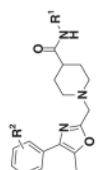
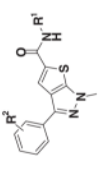
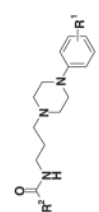
^bThe most active is reported for each family; family substructure shown in bold.

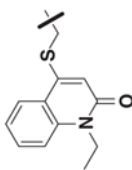
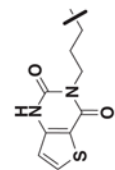
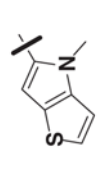
^cThe values refer to the associated AIDs. The biological activity of the best in class was profiled by structure in PubChem. Confirmatory includes only those compounds found active in confirmatory PubChem uploads with the number of prostate differentiation AIDs represented in parentheses.

Table 3

Ranked Active Compounds from Chemotype Families 1, 2, and 5

Compound	CID #	SID #	Scaffold	Chemotype Families			PC3 EC ₅₀ (μM)
				R ¹	R ²	LNCaP EC ₅₀ (μM)	
1	3240581	4246202	1				6.5 ^d
2	3239818	4245336	1				1.16 ^d
3	3244725	4250981	1				1.27
4	3245404	4251758	1				5.08 ^d
5	3235876	4240817	1				3.44
6	5307204	7964743	1				6.46
7	3244199	4250380	1				—
8	5308376	7966684	2				1.46 ^d

Compound	CID #	SID #	Scaffold	R ¹	R ²	LNCaP EC ₅₀ (μM)	PC3 EC ₅₀ (μM)
9	5309908	7969338	2				1.51 ^a
10	5308340	7966622	2			5.53	5.34
11	5309397	7968423	2			7.20 ^a	2.48 ^a
12	5309938	7969384	2			7.20 ^a	20.79
13	5307327	7964957	2			6.66	2.85 ^a
14	5308230	7966434	2			6.41	—
15	5308205	7966399	5	3-chloro		1.87	11.14

Compound	CID #	SID #	Scaffold	R ¹	R ²	LNCaP EC ₅₀ (μM)	PC3 EC ₅₀ (μM)
16	3242312	4248204	5	2-fluoro		8.92	9.05
17	3245527	4251898	5	4-methoxy		7.64	>30
18	3242909	4248889	5	4-methoxy		16.77	>30

CID, PubChem compound identification; SID, PubChem substance identification; R, region; LNCaP, lymph node cancer of the prostate human cell line; PC3, human prostate cancer cell line (derived from bone metastasis); EC₅₀, half maximal effective concentration.

⁴The 30 μM concentrations were associated with low event counts that were attributed to compound toxicity. The reported EC₅₀ calculation excluded values associated with a low event count. Dashed entries showed no activity at the tested concentration range or demonstrated low maximal effect.